Symmetry-induced singularities of the dispersion surface curvature and high sensitivities of a photonic crystal

Wei Jiang[1,2,*] and Ray T. Chen[1]
[1]*Department of Electrical and Computer Engineering and Microelectronics Research Center, University of Texas, Austin, Texas 78758, USA*
[2]*Department of Electrical and Computer Engineering and Institute for Advanced Materials, Devices, and Nanotechnology, Rutgers University, Piscataway, New Jersey 08854, USA*
(Received 11 October 2007; revised manuscript received 17 December 2007; published 6 February 2008)

We rigorously analyze the dispersion function and the curvature of the dispersion surface of a photonic crystal to explore the fundamental limit of its angular sensitivities. With insight gained from group theory, we find that symmetry induced degeneracy gives rise to a singular dispersion surface curvature and a nonvanishing group velocity simultaneously. Near such a singularity, high angular sensitivities can be achieved at low optical loss. This phenomenon exists generally in most common two-dimensional and three-dimensional photonic crystal lattices, although it occurs only for certain photonic bands as dictated by symmetry. This symmetry-induced effect is absent in one-dimensional crystals. Rigorous formulas of the sensitivities of the light beam directions to wavelength and refractive index changes are derived. Individual contributions of the dispersion surface curvature and group velocity to these sensitivities are separated. In the absence of the Van Hove singularity, a singular dispersion surface curvature gives rise to ultrahigh dispersion $|\frac{d\theta}{d\lambda}| > 10^3$ deg/nm and refractive index sensitivity $|\frac{d\theta}{dn_a}| > 10^4$ deg without compromising optical transmission. The angular dispersion value is significantly larger than those previously reported for the superprism effect and is not due to slow group velocity. We also discuss how various parameters intrinsic and extrinsic to a photonic crystal may suppress or enhance the angular sensitivities according to the rigorous formulas we obtain.

DOI: 10.1103/PhysRevB.77.075104 PACS number(s): 42.70.Qs, 07.07.Df, 42.65.−k, 61.50.Ah

I. INTRODUCTION

Photonic crystals provide high optical sensitivities not achievable in conventional media. The high dispersion and slow group velocity of photonic crystal waveguides help significantly shorten the interaction length for optical modulation.[1–5] Critical to this advance is a clear-cut expression that gives the enhancement of the nonlinear phase sensitivity of a photonic crystal waveguide mode in terms of the group velocity.[1] On the other hand, the high anisotropy and angular dispersion of photonic crystals were found to cause beam directions to have 500-fold higher sensitivities to wavelength variation, which was named the superprism effect.[5] Such high wavelength sensitivities are frequently accompanied by high sensitivities to refractive index perturbations.[6,7] These high sensitivities have aroused wide interest for potential applications in fiber optic communication, sensing, and nonlinear optics.[5–17] However, a general, quantitative relation between the anisotropy and these sensitivities of photonic crystals is needed to determine the ultimate limits of the sensitivities before we can fully uncover the potential of these sensitive effects for a wide range of important applications. For example, the sensitivity of the superprism effect is often enhanced near a band edge at the cost of a low optical transmission due to the slow group velocity. Whether this sets a fundamental limit of the maximum achievable sensitivity for practical applications is an interesting question to explore.

In this work, we rigorously show that high angular sensitivities to wavelength and refractive index perturbations can be achieved in the vicinity of a singular dispersion surface curvature *or* the vicinity of a vanishing group velocity. Explicit analytical expressions are given to separate the effects of the curvature and group velocity. Of particular interest is the case where a singular curvature appears together with a nonvanishing group velocity (and therefore high transmission) owing to symmetry-induced mode degeneracy. Such a case is predicted prevalent in high symmetry two-dimensional (2D) and 3D photonic crystal lattices, but absent in 1D photonic crystals. Van Hove singularities, the singularities of the density of states due to a vanishing group velocity, have been proven to be an insightful concept for understanding some interesting effects in photonic crystals.[18] The singularities of the dispersion surface curvature discussed here may occur at nonvanishing group velocities, where Van Hove singularities are absent. Therefore this type of singularity can lead us to some different effects or new functional regimes of photonic crystals.

This paper is organized as follows. In Sec. II A, we will first examine some analytic properties of the photonic crystal dispersion function. This allows us to identify the correlation and decorrelation of a singular curvature and a vanishing group velocity, which highly depends on lattice symmetry and mode degeneracy. An example based on an approximate model is presented in Sec. II B. In Sec. III, we give key rigorous formulas of the angular sensitivities of photonic crystals. An example is used to illustrate the individual control of the curvature and group velocity so as to achieve large sensitivities at low optical loss. Section IV discusses the contributions of intrinsic and extrinsic parameters to photonic crystal sensitivities, the effect of dimensionality and lattice types, and the difference from Van Hove singularities.

II. CURVATURE OF THE DISPERSION SURFACE AND GROUP VELOCITY

A. Some key analytic properties and symmetry considerations

For simplicity, we illustrate our ideas with the TM polarization (magnetic field in the plane) of a 2D photonic crystal. The field equation, according to Bloch theorem, can be written as

$$-(\mathbf{k}+\mathbf{G})^2 E(\mathbf{G}) + \omega^2 \sum_{\mathbf{G}'} \varepsilon(\mathbf{G}-\mathbf{G}')E(\mathbf{G}') = 0, \tag{1}$$

where $\mathbf{G}$ and $\mathbf{G}'$ are reciprocal lattice vectors, $\mathbf{k}$ is the wave vector, ε is the dielectric constant, and E is the electric field component normal to the plane. We have assumed the speed of light $c=1$ for convenience. Generally, the zeros of the secular determinant $D(k_x,k_y,\omega)$ of the eigenvalue problem Eq. (1) give the frequency ω as an *implicit* function of $\mathbf{k}$. Starting from this implicit dispersion function instead of an explicit $\omega(\mathbf{k})$ is essential to linking the mode degeneracy to a special type of curvature singularities of the dispersion surface.

To study the curvature, it is necessary to find the second-order expansion of D around an *arbitrary* point $\mathbf{k}_0$. A full Taylor expansion of D in terms of Δk_x, Δk_y involves many terms. We choose a *local* coordinate system (u,v) that gives a simpler expansion and a clear physical picture.[19]

Consider the expansion of the determinant $D(k_x,k_y,\omega)$ for a fixed frequency ω,

$$D(k_{x0}+u\cos\gamma - v\sin\gamma, k_{y0}+u\sin\gamma + v\cos\gamma, \omega) = \sum_{j=0}^{\infty} f_j(u,\omega)v^j = 0, \tag{2}$$

where the v axis of this local coordinate system is tangent to the dispersion contour at an arbitrary $\mathbf{k}_0$, i.e., $du/dv=0$; and γ is the angle between the u and x axes. Also, the u axis is parallel to the normal vector of the dispersion contour. Then the dispersion surface curvature,

$$\zeta \equiv \frac{\dfrac{d^2u}{dv^2}}{\left[1+\left(\dfrac{du}{dv}\right)^2\right]^{3/2}},$$

is simplified to

$$\zeta = \frac{d^2u}{dv^2}.$$

It is a simple exercise to show (see Appendix A)

$$\frac{du}{dv} = \left(\frac{\partial u}{\partial v}\right)_{\omega} = -\frac{f_1}{\partial f_0/\partial u} = 0, \tag{3a}$$

$$\zeta = \left(\frac{\partial^2 u}{\partial v^2}\right)_{\omega} = -\frac{2f_2}{\partial f_0/\partial u}, \tag{3b}$$

at $\mathbf{k}_0$ (i.e., $u=v=0$), hence $f_1(0,\omega)=0$ in this coordinate system. The group velocity components are given by

$$v_g = \frac{\partial\omega}{\partial u} = -\frac{\partial f_0/\partial u}{\partial f_0/\partial\omega}, \tag{4a}$$

$$\frac{\partial\omega}{\partial v} = -\frac{f_1}{\partial f_0/\partial\omega} \equiv 0. \tag{4b}$$

Comparing Eqs. (3b) and (4a), it is apparent that in the neighborhood of certain $\mathbf{k}_c$ where $(\partial f_0/\partial u)_{\mathbf{k}_c}=0$, a large curvature ζ and a slow group velocity v_g would appear simultaneously. For convenience of discussion, we introduce the group index $n_g=c/v_g$. The large values of ζ and n_g are generally correlated to each other through a common factor $(\partial f_0/\partial u)^{-1}$ in this neighborhood.

However, physically it is often undesirable to have a slow group velocity because it may cause high optical loss (details discussed later). Further inspection of Eq. (4a) indicates that a simultaneously vanishing $\partial f_0/\partial\omega$ could break the aforementioned correlation between ζ and n_g and give an arbitrarily large ζ without entailing a vanishingly small group velocity. At first glance, to simultaneously achieve $\partial f_0/\partial\omega=0$ and $\partial f_0/\partial u=0$ may require a photonic crystal to have specially designed structure parameters. However, we note that since the group velocity cannot exceed c due to causality, a vanishing $\partial f_0/\partial\omega$ always leads to a vanishing $\partial f_0/\partial u$ according to Eq. (4a), though not conversely. To trace the origin of $\partial f_0/\partial\omega=0$, we note an identity at $v=0$,

$$f_0(u,\omega) \equiv D(k_{x0}+u\cos\gamma, k_{y0}+u\sin\gamma, \omega) = 0.$$

Now one readily shows that $\partial f_0/\partial\omega=0$ (hence a singular ζ at $v_g\neq 0$) can be achieved if the dispersion function D has a degenerate mode at $\mathbf{k}_0$, i.e.,

$$D(k_{x0},k_{y0},\omega) = c_0(\omega-\omega_0)^n,$$

where the degree of degeneracy $n>1$.

It is well-known that degenerate eigenmodes will appear at certain high symmetry points of the Brillouin zone (BZ) where the associated little groups have at least one irreducible representation (IRREP) whose dimension is two or higher;[20,21] and the dimensionality of irreducible representations is known to play important roles in determining the physical properties of some photonic crystal structures of wide interests.[20–22] The K point of a triangular lattice is associated with a little group C_{3v}, which has two 1D irreducible representations A_1, A_2, and one 2D irreducible representation E.[20] Therefore the above analysis predicts that a singularity of ζ, together with a nonvanishing v_g, may appear at K for certain photonic bands.

B. Example and some approximate forms of the curvature on the BZ boundary

As an example, we study the dispersion surface curvature for a triangular lattice with parameters $n_a=3.8$, $n_b=1.33$, and

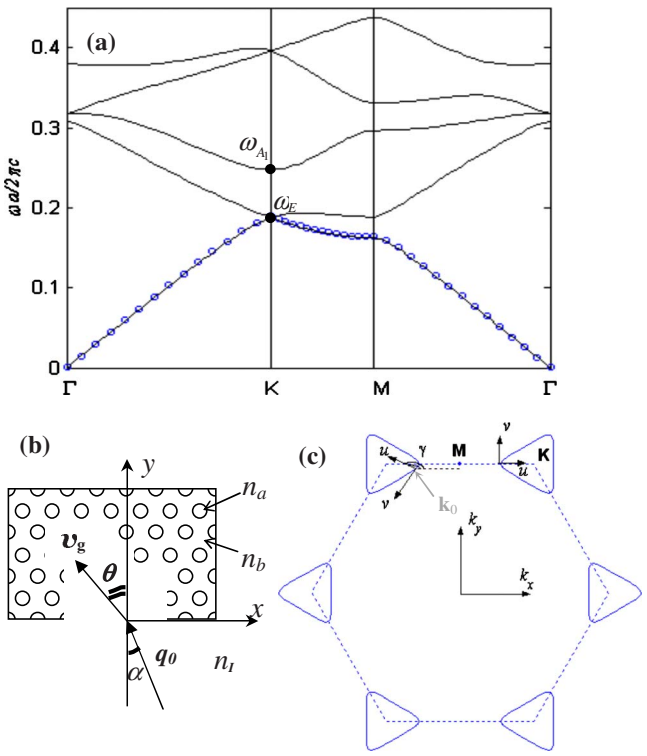

FIG. 1. (Color online) A triangular lattice. (a) Photonic bands for a structure: $n_a=3.8$, $n_b=1.33$; and $r=0.3a$; lines: PWE method; circles: DPT method. The two lowest bands have IRREPs E and A_1 at K. (b) Schematic of a typical experimental configuration. (c) A typical dispersion surface for the lower branch of the first band.

$r=0.3a$. Intuitively, the dispersion contour depicted in Fig. 1(c) shrinks as ω approaches ω_E; its curvature ζ (roughly the inverse of the radius) grows toward infinity for smaller and small contours. A close-up examination of the $\omega(k)$ curves in Fig. 1(a) shows that their slopes approach a nonvanishing value as ω approaches ω_E; this indicates nonvanishing v_g values. These intuitive pictures facilitate the qualitative understanding of the phenomena in this particular example. However, to prove that these effects mathematically follow from the theory given in the preceding section and therefore are a particular instance of a general effect proposed herein requires more detailed study.

In this section we employ a degenerate perturbation technique (DPT) involving three dominant Fourier components[23] to analytically compute ζ for this 2D triangular lattice. The numerical form of this DPT has been studied in detail.[23] Here we find that this DPT turns out to give some heuristic analytic forms of the curvature. As a by-product, we also find some interesting analytic forms of other physical quantities such as the frequencies at the band edge of high symmetry points. Note that this approximate DPT theory is used in this section (Sec. II B) only.

We have verified that this DPT method agrees well with the rigorous plane wave expansion (PWE) method for eigenfrequencies of the lowest band, as shown in Fig. 1(a). We define $\rho_0^2=\omega^2\varepsilon(0)$, $\rho_1^2=\omega^2\varepsilon(\mathbf{b}_1)=\omega^2\varepsilon(\mathbf{b}_2)=\omega^2\varepsilon(\mathbf{b}_3)$, where $\mathbf{b}_1$, $\mathbf{b}_2$, and $\mathbf{b}_3$ are the three shortest reciprocal lattice vectors and $\varepsilon(\mathbf{G})$ can be given in Bessel functions.[20] For this section only, we consider coordinates (u,v) with the origin fixed at the K point and $\gamma=0$, which allows for a simple analytic expression of ζ on the BZ boundary. The determinant D of Eq. (1) for the three leading Fourier components is given by

$$D=\begin{vmatrix} \rho_0^2-k^2 & \rho_1^2 & \rho_1^2 \\ \rho_1^2 & \rho_0^2-k_1^2 & \rho_1^2 \\ \rho_1^2 & \rho_1^2 & \rho_0^2-k_2^2 \end{vmatrix}=0,$$

where $\mathbf{k}=\mathbf{k}_c+u\mathbf{e}_x+v\mathbf{e}_y$, $\mathbf{k}_1=\mathbf{k}+\mathbf{b}_1$, and $\mathbf{k}_2=\mathbf{k}+\mathbf{b}_2$. We compute $f_0(u,\omega)$, and $f_2(u,\omega)$ from the secular determinant D according to Eq. (2),

$$f_0(u,\omega)=g_0g_1g_2-\rho_1^4(g_0+g_1+g_2)+2\rho_1^6, \tag{5a}$$

$$f_2(u,\omega)=-[g_0g_1+g_1g_2+g_0g_2+g_1b_2^2-3\rho_1^4], \tag{5b}$$

where $g_0=\rho_0^2-(k_{xc}+u)^2-b_2^2/4$, $g_1=\rho_0^2-(k_{xc}+u-b_{1x})^2$, and $g_2=g_0$. At K, we have

$$f_0(0,\omega)=(g_0-\rho_1^2)^2(g_0+2\rho_1^2)=0.$$

The first factor clearly indicates a doubly degenerate root,

$$\omega_{1,2}^2=b_2^2/[3\varepsilon(0)-3\varepsilon(\mathbf{b}_1)]=\omega_E^2,$$

at the K point. The other root is $\omega_3^2=b_2^2/[3\varepsilon(0)+6\varepsilon(\mathbf{b}_1)]$. Note $\varepsilon(\mathbf{b}_1)<0$ in this case.

The curvature ζ is computed via Eq. (3b) along MK for part of the first band below ω_E,

$$\zeta=-\frac{1}{u}\frac{\tilde{f}+b_2^2g_1}{\tilde{f}+b_2^2g_0}, \tag{6}$$

where $\tilde{f}(u,\omega)=g_0g_1+g_1g_2+g_0g_2-3\rho_1^4$. One readily verifies that $g_0=g_1=\rho_1^2$ for the degenerate mode at ω_E (where $u=0$). Therefore, on the MK line, the curvature has the asymptotic form $\zeta\to-1/u$ as $u\to0$. Furthermore, we note

$$\partial f_0/\partial u=-u(\tilde{f}+b_2^2g_0);$$

$$\partial f_0/\partial\omega=(2/\omega)[\rho_0^2\tilde{f}-2\rho_1^4(g_0+g_1+g_2-3\rho_1^2)].$$

One readily verifies $\partial f_0/\partial\omega\to\text{const}\times u$ as $u\to0$. Hence the cancellation according to Eq. (4a) gives a nonvanishing v_g at K. Thus, within the DPT framework, a singularity of ζ with a finite n_g is analytically verified for this example.

Figure 2 shows that the values of ζ and n_g obtained from the DPT method agree well with the PWE method. The logarithmic plot also reveals that the variation of ζ follows the group index n_g along most of the MK line except near K ($k_xa=1/3$), where a varnishing $\partial f_0/\partial\omega$ *breaks the correlation* between a singular ζ and a singular n_g, as predicted. The curvature in the entire BZ is plotted in Fig. 2 (inset) for the lower branch (below E) of the first band. The large ζ values on the BZ boundaries reflect the typical contour shape depicted in Fig. 1(c), where the dispersion contour bends abruptly across the BZ boundary. The curvature becomes singular at high symmetry points M ($k_xa=0$) and K. The normalized curvature $2\pi\zeta/\lambda$ for an ordinary medium is around unity, but it can be several orders of magnitude

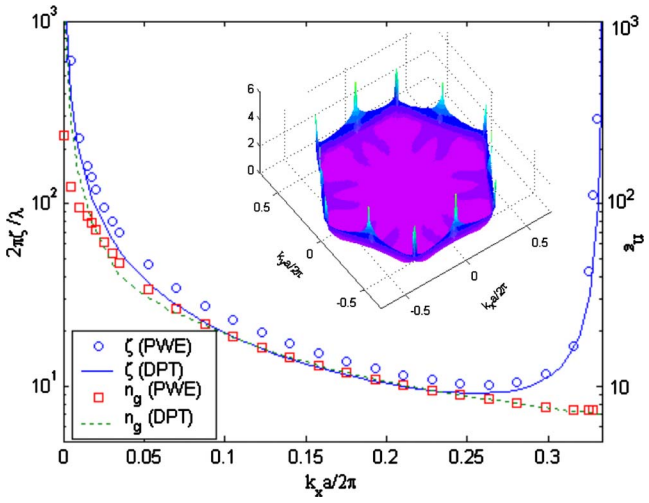

FIG. 2. (Color online) The dispersion surface curvature and group index on the *MK* line for the lower branch of the first band. The inset plots $\log_{10}(\frac{2\pi|\zeta|}{\lambda}+1)$ in the 1 BZ for this branch.

higher in photonic crystals. Note the DPT is used to give an intuitive expression of ζ for this example, it will not be employed in the derivation or calculation in the rest of this work.

III. ANGULAR SENSITIVITIES OF A PHOTONIC CRYSTAL

A. Derivation of the sensitivity formulas

The response of the mode energy flux direction (i.e., beam direction) of a photonic crystal to a small perturbation of wavelength or refractive index is of paramount interest to many applications. To study this optical response, we need to find the relationship between ζ and a measurable (extrinsic) quantity in a typical experimental configuration illustrated in Fig. 1(b). The coupling condition for the input surface is given by

$$n_I\omega \sin\alpha = k_{x0} + u\cos\gamma - v\sin\gamma, \tag{7}$$

where γ is the angle of the group velocity at $\mathbf{k}_0 = k_{x0}\mathbf{e}_x + k_{y0}\mathbf{e}_y$ with respect to the input interface. Here $\mathbf{k}_0$ is an arbitrary point on an arbitrary dispersion contour. Consider cases where the incident angle, α, is fixed and one varies the wavelength or the refractive index of one constituent material (for example, n_a).

First, we analyze the wavelength perturbation. We notice

$$\Delta u = \left(\frac{\partial u}{\partial \omega}\right)_v \Delta\omega + \left(\frac{\partial u}{\partial v}\right)_\omega \Delta v + \cdots = \left(\frac{\partial u}{\partial \omega}\right)_v \Delta\omega + \cdots, \tag{8}$$

where we have omitted terms of the order $\Delta\omega^2$, Δv^2, $\Delta\omega\Delta v$, and higher. The second term in Eq. (8) vanishes because we have $(\partial u/\partial v)_\omega = 0$ along a dispersion contour (constant-ω contour). We also note that according to Eq. (7), a perturbation $\Delta\omega$ with a fixed value of α leads to

$$n_I\Delta\omega\sin\alpha = k_{x0} + \Delta u\cos\gamma - \Delta v\sin\gamma$$

around $u=v=0$. Note in the above equation, terms proportional to $\Delta\gamma$ vanish at $u=v=0$ and should not appear. By virtue of Eq. (8), one readily shows

$$\frac{\Delta v}{\Delta\omega} = \frac{-1}{\sin\gamma}\left[n_I\sin\alpha - \left(\frac{\partial u}{\partial\omega}\right)_v\cos\gamma\right]. \tag{9}$$

Note the higher order terms omitted in Eq. (8) have vanishing contributions in Eq. (9) in the limit $\Delta\omega\to 0$; hence they are not shown. The derivative $(\partial u/\partial\omega)_v$ is just the group index, n_g (note $c=1$ in this paper). Also, by definition of the curvature, we have $|\Delta\theta/\Delta v| = |\zeta|$. Hence, by virtue of Eq. (9), the wavelength sensitivity is given by

$$\left|\frac{d\theta}{d\omega}\right| = \left|\frac{d\theta}{dv}\frac{dv}{d\omega}\right| = \left|\frac{\zeta}{\cos\theta}(n_I\sin\alpha - n_g\sin\theta)\right|. \tag{10}$$

Note $\theta = \frac{\pi}{2} - \gamma$ [note Figs. 1(b) and 1(c) illustrate a case of $\theta<0$, $\alpha<0$].

Now we study the perturbation of refractive index. A perturbation of Δn_a at a fixed ω results in

$$\frac{\Delta u}{\Delta n_a}\cos\gamma = \frac{\Delta v}{\Delta n_a}\sin\gamma$$

according to Eq. (7). The refractive index sensitivity can be calculated from $\frac{d\theta}{dn_a} = \frac{\Delta\theta}{\Delta v}\frac{\Delta v}{\Delta n_a}$, which gives

$$\left|\frac{d\theta}{dn_a}\right| = \left|\frac{\zeta}{\cos\theta}\left[\sin\theta\left(\frac{\partial u}{\partial n_a}\right)_{\omega,v}\right]\right|. \tag{11}$$

Using the Jacobian determinants, one readily shows that

$$\left(\frac{\partial u}{\partial n_a}\right)_{\omega,v} = -\left(\frac{\partial\omega}{\partial n_a}\right)_{u,v}\left(\frac{\partial u}{\partial\omega}\right)_{n_a,v},$$

where the second term on the right side is just the group index, n_g (note $c=1$). Now we find that the angular sensitivity to a refractive index perturbation (for a fixed incident angle and fixed wavelength) is given by

$$\left|\frac{d\theta}{dn_a}\right| = \left|-\zeta\tan\theta\left(\frac{\partial\omega}{\partial n_a}\right)_{\mathbf{k}} n_g\right|. \tag{11'}$$

One can compute $(\partial\omega/\partial n_a)_{u,v} \equiv (\partial\omega/\partial n_a)_{\mathbf{k}}$ easily by varying n_a in the photonic band calculation. Note that except for angles θ, α, and n_I, other quantities in Eqs. (10) and (11′) are intrinsic properties of a photonic crystal, independent of the choice of the coordinate system and the crystallographic orientation of the input surface. According to Eqs. (10) and (11′), the sensitivities to wavelength and index perturbations can be enhanced by a large dispersion surface curvature or by a large group index. A key feature of Eqs. (10) and (11′) is that high sensitivities to wavelength and refractive index perturbations are usually correlated, through common terms ζ and n_g.

B. Individual control of the curvature and the group velocity

However, it turns out that a large value of n_g results in low transmission, and therefore enhancing ζ is practically a better

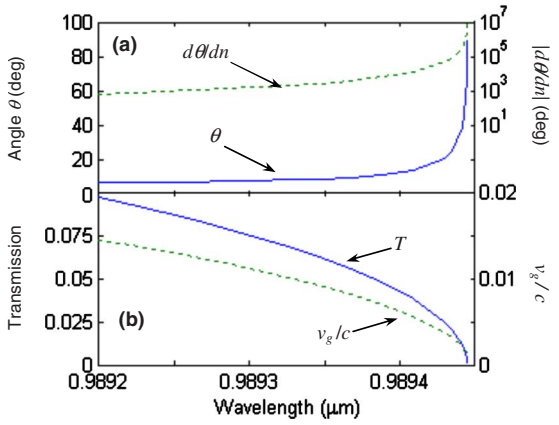

FIG. 3. (Color online) Normalized transmission and sensitivities for modes near the K-valley of the second band, $\omega_{A_1}a/2\pi c \sim 0.248$, $\alpha=20.8°$, $n_1=n_a$.

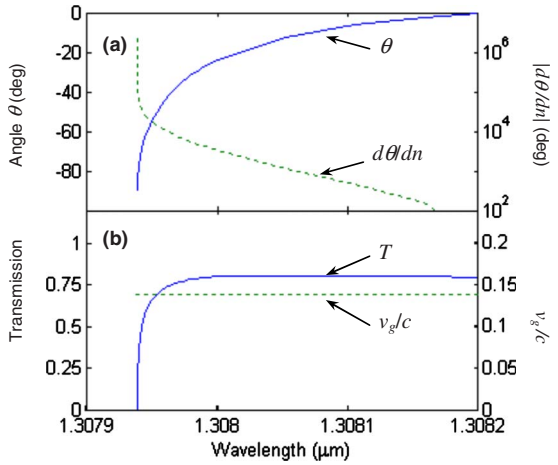

FIG. 4. (Color online) Normalized transmission and sensitivities for modes near the degenerate ω_E mode of the first band, $\omega_E a/2\pi c \sim 0.187$, $\alpha=27.9°$, $n_I=n_a$.

approach to ultrahigh sensitivities. According to our previous theory on surface coupling,[24] the normalized transmission is given by the ratio of the surface-normal component of the Poynting vector $S_y \sim \varepsilon_{em} v_g \cos\theta$,

$$T \sim |t|^2 \varepsilon_{em} v_g \cos\theta, \tag{12}$$

where ε_{em} is the mode energy density and t is the complex coupling amplitude[24] of the mode in question. Typically, the wavelength or refractive index varies over an ultranarrow range (less than ~1%) in high sensitivity cases, and $|t|$ and ε_{em} generally vary insignificantly across this range according to our computation. For the modes in the nondegenerate K-valley (IRREP A_1) in Fig. 1(a), the group velocity v_g vanishes as the wavelength approaches the band edge at ω_{A_1}. Thus the normalized transmission T is low, and T largely follows the trend of small v_g as shown in Fig. 3(b) in accordance to Eq. (12). High sensitivities, $|\frac{d\theta}{dn_a}|$, shown in Fig. 3(a) are achieved at the cost of low transmission. In contrast, the symmetry-induced degeneracy limits v_g to a nonvanishing value around the degenerate K point (IRREP E) at ω_E. Therefore the transmission remains high for most of the spectrum as depicted in Fig. 4(b).

To recapitulate, we note that the sensitivities to wavelength and refractive index can be significantly enhanced if any of the three terms, ζ, n_g, and $1/\cos\theta$, is large in Eqs. (10) and (11′). Unfortunately, the transmission given in Eq. (12) is inversely proportional to the last two terms, leaving ζ the only desired route for high sensitivities at low optical loss.

For a numerical example, we set the transmission threshold at 50%. This gives the maximum achievable $|\frac{d\theta}{d\lambda}| \sim 3 \times 10^3$ deg/nm and $|\frac{d\theta}{dn_a}| \sim 3.5 \times 10^4$ deg near the degenerate K point at ω_E in the first band, according to Fig. 4(a). Clearly, orders of magnitude higher sensitivities can be achieved in a photonic crystal without severely suppressing optical transmission. Here we are more interested in index sensitivities for sensing and nonlinear optics applications. These applications do not require the beam center shift to be much larger than the beam width, and therefore are not limited by some issues found in wavelength demultiplexing applications.[10] Generally, it is easy to detect a minimum lateral shift 10 μm of the beam center on the exit end of a photonic crystal. Then a photonic crystal sensor only needs a length <50 μm to resolve a refractive index change of $\Delta n_a \sim 0.001$ with a sensitivity $|\frac{d\theta}{dn_a}| \sim 10^4$ deg. A high $|\frac{d\theta}{dn_a}|$ value may also significantly enhance certain nonlinear optical effects such as all optical switching and beam-steering[7] or deflection based Q-switching, where a small Δn_a can be generated by a pump-control beam or by the signal beam itself. Detailed discussion on applications is beyond the scope of this paper.

IV. DISCUSSIONS

A. Intrinsic and extrinsic parameters

All quantities in Eqs. (10) and (11′) can be easily calculated in any coordinate system. For example, $(\partial\omega/\partial n_a)_{u,v} \equiv (\partial\omega/\partial n_a)_{\mathbf{k}}$, the latter can be computed in a regular (k_x,k_y) coordinate system whose origin is at the BZ center, Γ. Also, the well-known formulas, $\zeta \equiv \frac{d^2k_y}{dk_x^2}/\left[1+\left(\frac{dk_y}{dk_x}\right)^2\right]^{3/2}$ and $n_g = c/|\nabla_k\omega|$, can be employed to calculate ζ and n_g in (k_x,k_y) coordinates. Indeed, it is straightforward to see that these intrinsic quantities $[|\zeta|, n_g$, and $(\partial\omega/\partial n_a)_{\mathbf{k}}]$ do not rely on the choice of the coordinate systems. Note this statement is valid only for those coordinate systems that can be related to (k_x,k_y) through a Euclidian transformation, which is sufficient for all practical purposes. As long as the values of ζ, $(\partial\omega/\partial n_a)_{u,v}$, and n_g are computed for each $\mathbf{k}$ point separately, we will not compromise the rigor of Eqs. (10) and (11′). More discussion on understanding the rigor of our method is presented in Appendix B.

We call θ and α extrinsic parameters because they are related to how a photonic crystal is coupled on the surface. The angle θ should be determined as the angle of the group velocity at the coupled $\mathbf{k}_0$ point with respect to the normal of the photonic crystal surface. Therefore if we rotate the x,y

axes (but not lattice axes intrinsic to the photonic crystal), the angle θ should not change.

Some further analysis helps understand the effects of intrinsic and extrinsic parameters. Once a coupling configuration (including surface orientation, incident angle, and wavelength) is given, the sensitivity values given in Eqs. (10) and (11′) are determined, independent of the choice of the coordinate system. On the other hand, consider two experiments for the same photonic crystal lattice: (1) light impinges on a surface having Miller indices $(h_1h_2)=(10)$ at an incident angle α_1; and (2) light impinges on a surface having $(h_1h_2)=(23)$ at an incident angle α_2. By coincidence we may couple to the same (physical) $\mathbf{k}_0$ point on the dispersion surface in these two experiments. Although the intrinsic parameters ζ, $(\partial\omega/\partial n_a)_{u,v}$, and n_g are the same, the different extrinsic parameters cause entirely different angular sensitivity values. In this sense, these angular sensitivities themselves are also extrinsic quantities, which depend on the external coupling conditions.

The separation of extrinsic parameters and intrinsic parameters also allows us to see some interesting effects. Generally, a large intrinsic parameter ζ at a photonic band of interest means that a photonic crystal is potentially highly sensitive to both wavelength and refractive index perturbations. However, the external coupling conditions, described by the extrinsic parameters, could modify or even suppress certain sensitivities actually observed. For example, if the term $n_I \sin\alpha - n_g \sin\theta$ in Eq. (10) vanishes under a given coupling configuration (or close to zero over a range of coupling parameters), it is possible to produce a device that has a very high refractive index sensitivity and a relatively low wavelength sensitivity in certain parameter ranges. This may help enhance the bandwidth of certain devices. Further study is needed to explore this possibility.

B. Effects of dimensionality and lattice types

The theory developed here can be extended to treat other common lattices in 2D and 3D. We note that a similar singularity of ζ can occur for a square lattice, where the corresponding BZ corner (M point) retains the C_{4v} symmetry and has one 2D irreducible representation. Therefore an ultralarge curvature can appear with a nonvanishing v_g for the two most common 2D lattice types. Similar analysis can be applied to the TE polarization. It can be proven from group theory that symmetry-induced singularities of the dispersion surface curvature at $v_g \neq 0$ can also exist for most common 3D lattices, such as simple-cubic, face-centered-cubic, and body-centered-cubic lattices. The analysis will be similar in spirit though more complicated in form because a surface in 3D has two principal curvatures.[19] For many practical scenarios in 3D, effective 2D dispersion surfaces may be used,[5] then the above 2D analysis remains applicable.

The phenomena discussed here do not exist in 1D photonic crystals because all 1D point groups are Abelian and have no degeneracy. For a 1D grating of the same period a, its angular dispersion[25] $\frac{d\theta}{d\lambda} \sim \frac{1}{a\cos\theta}$ is much lower (<0.2 deg/nm) for any reasonable value of θ. The preceding high $\frac{d\theta}{d\lambda}$, $\frac{d\theta}{dn_a}$ values of the 2D lattice are obtained at $|\theta| < 70°$ with negligible contribution from the $\frac{1}{\cos\theta}$ factor in Eqs. (10) and (11′).

Note that our photonic crystal surface coupling theory[24] has been extended to compute mode transmissions for 3D photonic crystals[26] and 1D gratings.[27] Also note that in grating diffraction, the diffracted beam angle refers to the angle outside the grating. For the original superprism effect, the beam angle sensitivity refers to the angle inside the photonic crystal. For some integrated devices,[15] beam angles outside the photonic crystal need not be sensitive and the sensitivity is employed through the sensitive shift of the output position on the exit surface. If the output angle sensitivity is exploited, then the output surface must not be parallel to the input surface.[12,14]

C. Van Hove singularities and some other issues

We shall mention that Van Hove envisioned that a minimum of one band and a maximum of another may "contact" each other, and the Van Hove singularity will be weakened or suppressed by "compensation."[28] In our case, it is straightforward to prove that the Van Hove singularity is virtually absent[29] at ω_E due to a nonvanishing v_g, but the curvature ζ exhibits a singularity. Note that one type of extreme anisotropy near the Γ point was found to be associated with a divergent Van Hove singularity for a 2D square lattice.[30] The curvature singularity discussed here comes with a suppressed Van Hove singularity, and is a different, *general* phenomenon. Our Eq. (10) shows $\frac{d\theta}{d\omega} \propto \zeta$ and may also shed new light on some issues for $\zeta=0$.

Note that usually the dielectric function of a photonic crystal is local and is considered accurately known. Hence additional boundary conditions[31] are not needed for a semi-infinite photonic crystal even when multiple modes appear. Other theoretical works on photonic crystal surface coupling also do not invoke additional boundary conditions.[32]

In summary, we rigorously analyze the dispersion surface curvature in 2D photonic crystals and discuss its relation to angular sensitivities of a photonic crystal. The individual contributions of the curvature and group index to the angular sensitivities are separated. Furthermore, assisted by group theory, we analytically show that symmetry induced degeneracy allows for high sensitivities without compromising optical transmission in 2D and 3D photonic crystals, leading to promising applications including sensing and nonlinear optics. We also discuss the possibility of maximizing the refractive index sensitivity while suppressing the wavelength sensitivity.

ACKNOWLEDGMENTS

We thank Nicholas X. Fang, R. L. Nelson, J. Haus, and Tao Ling for helpful scientific-technical discussions. We are also grateful to many colleagues and friends for kind encouragement and support. This work was supported by Air Force Research Laboratory under Grant No. FA8650-06-C-5403. Partial support from AFOSR (Grant No. FA9550-05-C-0171) and NASA (Grant No. NNX07CA84P) is acknowledged.

APPENDIX A: DERIVATIVES IN A LOCAL COORDINATE SYSTEM

By virtue of Eq. (2), the total derivative of D with respect to v along a constant-ω contour is given by

$$0 = \left.\frac{dD}{dv}\right|_{\omega} = \sum_{j=0}^{\infty} \frac{\partial f_j}{\partial u}\frac{du}{dv} v^j + \sum_{j=1}^{\infty} f_j(u,\omega) j v^{j-1}. \quad \text{(A1)}$$

At the origin of this local coordinate system (u,v), we have $v=0$. Hence Eq. (A1) is reduced to

$$\frac{\partial f_0}{\partial u}\frac{du}{dv} + f_1 = 0, \quad \text{(A2)}$$

from which we obtain Eq. (3a). Further differentiation of Eq. (A1) with respect to v yields

$$0 = \left.\frac{d^2D}{dv^2}\right|_{\omega} = \sum_{j=0}^{\infty} \left[\frac{\partial^2 f_j}{\partial u^2}\left(\frac{du}{dv}\right)^2 v^j + \frac{\partial f_j}{\partial u}\frac{d^2u}{dv^2} v^j \right] + \sum_{j=1}^{\infty} \frac{\partial f_j}{\partial u}\frac{du}{dv} j v^{j-1} + \sum_{j=1}^{\infty} \frac{\partial f_j}{\partial u}\frac{du}{dv} j v^{j-1} + \sum_{j=2}^{\infty} f_j(u,\omega) j(j-1) v^{j-2}. \quad \text{(A3)}$$

Here the first two sums come from the differentiation of the first sum in Eq. (A1), the last two sums from the second sum in Eq. (A1). At the origin of this local coordinate system (u,v), we have $v=0$, and $du/dv=0$. Hence Eq. (A3) is reduced to

$$0 = \frac{\partial f_0}{\partial u}\frac{d^2u}{dv^2} + 2f_2, \quad \text{(A4)}$$

from which we obtain Eq. (3b). By considering the total derivatives of D with respect to u and v along constant-v and constant-u lines respectively, Eqs. (4a) and (4b) can be proved similarly.

APPENDIX B: RIGOROUS NATURE OF THE SENSITIVITY FORMULAS

To understand the rigorous nature of Eqs. (10) and (11′), we point out some key features of our derivation. First, the origin of the local coordinate system is an *arbitrary* point $\mathbf{k}_0$ (not necessarily a high symmetry point). Second, in deriving these relations, we have not assumed a finite Fourier series. Third, the local expansion with respect to u,v is rigorous at $\mathbf{k}_0$ only. For another point $\mathbf{k}_0'$, no matter how close it is to $\mathbf{k}_0$, another local expansion with another set of local coordinates (u',v') must be used. In this way, the rigor of Eqs. (10) and (11′) is not compromised. Lastly, to compute the beam angle change due to a *finite* change of refractive index, the rigorous way is to integrate $\partial\theta/\partial n_a$ given by Eq. (11′) over the finite span of Δn_a.

The preceding procedure that involves local coordinates (u,v), although useful in understanding the rigor of Eqs. (10) and (11′), is somewhat complicated in practical calculations. Fortunately, we have simplified the sensitivity forms such that all quantities in Eqs. (10) and (11′) can be easily calculated in any coordinate systems. The details have been discussed in Sec. IV A. Note that, in contrast, Eq. (11) involves $(\partial u/\partial n_a)_{\omega,v}$, which is much less intuitive for direct computation in any coordinate systems. As long as the values of ζ, $(\partial\omega/\partial n_a)_{u,v}$, and n_g are computed for each $\mathbf{k}$ point individually, we will not compromise the rigor of Eqs. (10) and (11′). Lastly, even though the equations given are rigorous, the values of quantities such as ω and $\cos\theta$ entering Eqs. (10) and (11′) are usually approximated in numerical calculations due to a finite cutoff of the series used in computing ω and the cosine function. Nonetheless, rigorous equations with simple forms like Eqs. (10) and (11′) serve at least two important purposes. First, they single out a few key factors (e.g., ζ, n_g) that affect sensitivities. Such physical insight helps us easily identify the high sensitivity regimes of interest and avoid an aimless search in a large design space. Second, it provides *a priori* information of various quantities near numeric singularities (e.g., singular ζ). Generally such *a priori* information is invaluable in numeric calculations and helps us design numeric schemes that are highly accurate, reliable, and efficient near singularities.[33] We have employed at least 121 Fourier components to ensure better than 1% convergence for sensitivities.[34]

*wjiangnj@ece.rutgers.edu

[1] M. Soljacic, S. G. Johnson, S. H. Fan, M. Ibanescu, E. Ippen, and J. D. Joannopoulos, J. Opt. Soc. Am. B **19**, 2052 (2002); M. Soljacic and J. D. Joannopoulos, Nat. Mater. **3**, 211 (2004).
[2] Y. A. Vlasov, M. O'Boyle, H. F. Hamann, and S. J. McNab, Nature (London) **438**, 65 (2005).
[3] Y. Jiang, W. Jiang, L. Gu, X. Chen, and R. T. Chen, Appl. Phys. Lett. **87**, 221105 (2005).
[4] L. Gu, W. Jiang, X. Chen, L. Wang, and R. T. Chen, Appl. Phys. Lett. **90**, 071105 (2007).
[5] H. Kosaka, T. Kawashima, A. Tomita, M. Notomi, T. Tamamura, T. Sato, and S. Kawakami, Phys. Rev. B **58**, R10096 (1998).
[6] T. Prasad, V. Colvin, and D. Mittleman, Phys. Rev. B **67**, 165103 (2003); T. Prasad, D. M. Mittleman, and V. L. Colvin, Opt. Mater. (Amsterdam, Neth.) **29**, 56 (2006).
[7] N. C. Panoiu, M. Bahl, and R. M. Osgood, Opt. Lett. **28**, 2503 (2003).
[8] M. Notomi, Phys. Rev. B **62**, 10696 (2000).
[9] J. Bravo-Abad, T. Ochiai, and J. Sanchez-Dehesa, Phys. Rev. B **67**, 115116 (2003).
[10] T. Baba and T. Matsumoto, Appl. Phys. Lett. **81**, 2325 (2002).
[11] M. J. Steel, R. Zoli, C. Grillet, R. C. McPhedran, C. M. de Sterke, A. Norton, P. Bassi, and B. J. Eggleton, Phys. Rev. E **71**, 056608 (2005).
[12] L. Wu, M. Mazilu, T. Karle, and T. F. Krauss, IEEE J. Quantum Electron. **38**, 915 (2002).

[13] J. J. Baumberg, N. M. B. Perney, M. C. Netti, M. D. C. Charlton, M. Zoorob, and G. J. Parker, Appl. Phys. Lett. **85**, 354 (2004).
[14] A. Lupu, E. Cassan, S. Laval, L. El Melhaoui, P. Lyan, and J. M. Fedeli, Opt. Express **12**, 5690 (2004).
[15] B. Momeni, J. D. Huang, M. Soltani, M. Askari, S. Mohammadi, M. Rakhshandehroo, and A. Adibi, Opt. Express **14**, 2413 (2006).
[16] X. Yu and S. Fan, Phys. Rev. E **70**, 055601(R) (2004).
[17] J. Serbin and M. Gu, Adv. Mater. (Weinheim, Ger.) **18**, 221 (2006).
[18] See, for example, M. Ibanescu, E. J. Reed, and J. D. Joannopoulos, Phys. Rev. Lett. **96**, 033904 (2006); A. Mekis, M. Meier, A. Dodabalapur, R. E. Slusher, and J. D. Joannopoulos, Appl. Phys. A: Mater. Sci. Process. **69**, 111 (1999).
[19] Note many relations regarding the local tangent vector, normal vector, and curvature can also be elegantly treated using tensor notations in curvilinear coordinates, see, for example, D. F. Lawden, *Introduction to Tensor Calculus, Relativity, and Cosmology*, 3rd ed. (Wiley, New York, 1982). However, such notations are not frequently used in photonic crystal research. Also, note that the local coordinate system introduced here is slightly different from (global) curvilinear coordinates.
[20] K. Sakoda, *Optical Properties of Photonic Crystals* (Springer, Berlin, 2001).
[21] O. Painter, R. K. Lee, A. Scherer, A. Yariv, J. D. O'Brien, P. D. Dapkus, and I. Kim, Science **284**, 1819 (1999); O. Painter and K. Srinivasan, Phys. Rev. B **68**, 035110 (2003).
[22] W. Jiang and R. T. Chen, Phys. Rev. Lett. **91**, 213901 (2003).
[23] N. Malkova, S. Kim, T. DiLazaro, and V. Gopalan, Phys. Rev. B **67**, 125203 (2003).
[24] W. Jiang, R. T. Chen, and X. Lu, Phys. Rev. B **71**, 245115 (2005).
[25] J. Qiao, F. Zhao, J. Liu, and R. T. Chen, IEEE Photonics Technol. Lett. **12**, 1070 (2000).
[26] X. N. Chen, W. Jiang, J. Q. Chen, and R. T. Chen, J. Lightwave Technol. **25**, 2469 (2007).
[27] W. Jiang and R. T. Chen, J. Opt. Soc. Am. A **23**, 2192 (2006).
[28] L. Van Hove, Phys. Rev. **89**, 1189 (1953).
[29] *Mathematically*, the density of states $\rho(\omega)$ may have a removable singularity at ω_E; it can be removed by redefining $\rho(\omega_E)$.
[30] Y. A. Urzhumov and G. Shvets, Phys. Rev. E **72**, 026608 (2005).
[31] V. M. Agranovich and V. L. Ginzburg, *Crystal Optics with Spatial Dispersion and Excitons* (Springer, Berlin, 1984).
[32] E. Istrate, A. A. Green, and E. H. Sargent, Phys. Rev. B **71**, 195122 (2005); E. Istrate and E. H. Sargent, Rev. Mod. Phys. **78**, 455 (2006).
[33] G. Dahlquist and A. Bjorck, *Numerical Methods* (translated by N. Anderson) (Prentice-Hall, Englewood Cliffs, NJ, 1974).
[34] This work was first presented by W. Jiang, in *Air Force Workshop on Electro-optic Beam Steering* (Dayton, Ohio, 2007).